

# Extracting source parameters from beam monitors on a chopper spectrometer

D.L. Abernathy<sup>1,a</sup>, J.L. Niedziela<sup>2</sup> and M.B. Stone<sup>1</sup>

<sup>1</sup>Quantum Condensed Matter Division, Oak Ridge National Laboratory, Oak Ridge, Tennessee 37831, USA

<sup>2</sup>Instrument and Source Division, Oak Ridge National Laboratory, Oak Ridge, Tennessee 37831, USA

**Abstract.** The intensity distributions of beam monitors in direct-geometry time-of-flight neutron spectrometers provide important information about the instrument resolution. For short-pulse spallation neutron sources in particular, the asymmetry of the source pulse may be extracted and compared to Monte Carlo source simulations. An explicit formula using a Gaussian-convolved Ikeda-Carpenter distribution is given and compared to data from the ARCS instrument at the Spallation Neutron Source.

## 1. Introduction

Understanding the resolution of a neutron scattering spectrometer is critical for experimental planning, distinguishing scattering features of interest from resolution effects, and quantitative evaluation of the sample scattering function. The asymmetry in time of neutron production from short-pulse spallation sources is a feature of many direct geometry spectrometers, specifically those which do not employ a pulse-shaping chopper. The time structure of the neutrons emerging from a moderator at a given energy has a sharp rise after the protons hit the target followed by a slower decay and is generally describeable in terms of a fast and a slow time constant. Ikeda and Carpenter introduced a form for this pulse shape based on considerations of a short spallation neutron pulse driving a moderator and reflector system exhibiting a response with two time constants [1]. This pulse propagates through the spectrometer, modified by the instrument components, the sample scattering, and detection processes. As these independent interactions are generally symmetric, or at least limited in duration in the case of the detectors, the overall instrument response may be characterized by a Gaussian representation. Because of the extended time structure of the source, it is important to carry the source asymmetry through the analysis of the total instrument response and resolution characterization.

This process is also represented in the pulse shape of the beam monitors installed along the neutron path. Such monitors provide additional views of the evolving neutron pulse at different locations, and the information complements the typical resolution characterization done using an incoherent (vanadium) sample in the spectrometer. Figure 1 illustrates this principle on a timing diagram showing the pulse shape as a function of time-of-flight at different distances along the beamline. A first monitor at a distance  $L_{m1}$  from the source

placed just after the fast (Fermi) chopper at  $L_{fermi}$  provides information about the chopper's pulse time distribution. A second monitor at  $L_{m2}$  placed far downstream of the sample position shows more clearly the source term. As shown in Fig. 1, the brief opening of the chopper acts as a pinhole that inverts the source pulse shape in time. An analysis of the second monitor data, including the broadening effects of the chopper, provides parameters that may be scaled to reflect the effective time pulse at the source.

The Ikeda-Carpenter function is introduced in Sect. 2 and a Gaussian-broadened version is derived. In Sect. 3 this is applied to monitor data from the ARCS instrument at the Spallation Neutron Source (SNS) [2]. Source parameters as a function of nominal incident energy are found and compared to a characterization of the instrument resolution using vanadium scattering as well as Monte Carlo simulations of the source. A discussion of the results and conclusion are provided in Sect. 4.

## 2. The Gaussian-broadened Ikeda-Carpenter function

The time distribution of neutrons generated by a spallation neutron source moderator may be modeled by the Ikeda-Carpenter function [1]

$$i(t) = \frac{\alpha}{2} \left\{ (1-R)\alpha^2 t^2 e^{-\alpha t} + \frac{2R\alpha^2 \beta}{(\alpha - \beta)^3} \times \left[ e^{-\beta t} - e^{-\alpha t} \left( 1 + (\alpha - \beta)t + \frac{1}{2}(\alpha - \beta)^2 t^2 \right) \right] \right\} \quad (1)$$

for  $t > 0$ . The parameters  $\alpha$  and  $\beta$  are the inverse time constants of fast and slow processes respectively in the neutron moderator and reflector system. The form is inspired [1] by considering a fast moderation of the spallation neutrons with a time constant  $\tau_f = 1/\alpha$ , also

<sup>a</sup> e-mail: [abernathydl@ornl.gov](mailto:abernathydl@ornl.gov)

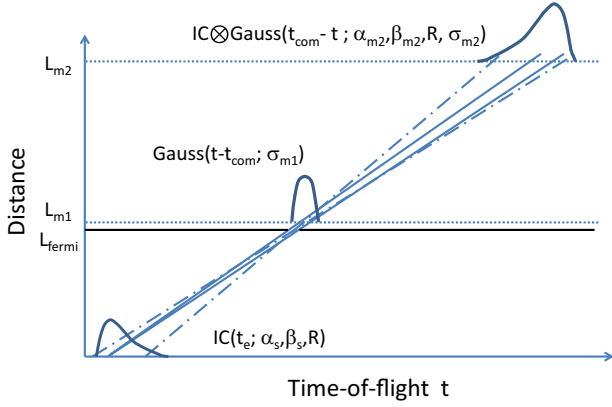


**Figure 1.** Timing diagram for a direct-geometry spectrometer illustrating the time-of-flight pulse shape evolution along the beamline.

known as the “slowing-down” term. The moderator is also driven by reflected neutrons in a slower process with time constant  $\tau_s = 1/\beta$ , giving rise to the “storage” term. The parameter  $0 < R < 1$  is a trade-off between the two components. The parameters change as a function of the neutron energy emerging from the moderator face. Note that the Ikeda-Carpenter function is normalized to unity when integrated over the range  $0 < t < \infty$ . Calculation of the mean emission time  $\bar{t}_e$  of the neutrons from Eq. (1) gives

$$\bar{t}_e = \frac{3}{\alpha} + \frac{R}{\beta}. \quad (2)$$

Since the instrument response function may often be well characterized by a Gaussian approximation, it is useful to calculate the convolution of the Ikeda-Carpenter function (Eq. (1)) with a Gaussian distribution [3]

$$G(t) = \frac{1}{\sqrt{2\pi}\sigma_G} e^{-\frac{t^2}{2\sigma_G^2}}, \quad -\infty < t < \infty, \quad (3)$$

to give the Gaussian-broadened distribution

$$i_G(t) = \int_{-t}^{\infty} i(t + \tau)G(\tau)d\tau \quad (4)$$

where the lower limit of integration is determined by the allowed range of the Ikeda-Carpenter function. Substituting Eqs. (1) and (3) and gathering like terms in the integration variable  $\tau$ , one finds that

$$\begin{aligned} i_G(t) = & \frac{\alpha}{2\sqrt{2\pi}\sigma_G} \left\{ \left[ (1-R)\alpha^2 t^2 - \frac{2R\alpha^2\beta}{(\alpha-\beta)^3} \right. \right. \\ & \left. \left. \left( 1 + (\alpha-\beta)t + \frac{1}{2}(\alpha-\beta)^2 t^2 \right) \right] e^{-\alpha t} g_0(\alpha, \sigma_G, t) \right. \\ & + \frac{2R\alpha^2\beta}{(\alpha-\beta)^3} e^{-\beta t} g_0(\beta, \sigma_G, t) \\ & + \left[ 2(1-R)\alpha^2 t - \frac{2R\alpha^2\beta}{(\alpha-\beta)^2} (1 + (\alpha-\beta)t) \right] \\ & \times e^{-\alpha t} g_1(\alpha, \sigma_G, t) \\ & \left. + \left[ (1-R)\alpha^2 - \frac{R\alpha^2\beta}{(\alpha-\beta)} \right] e^{-\alpha t} g_2(\alpha, \sigma_G, t) \right\} \quad (5) \end{aligned}$$

where the functions  $g_n$  are defined by the integral equation

$$g_n(x, \sigma_G, t) \equiv \int_{-t}^{\infty} \tau^n e^{-x\tau} e^{-\frac{\tau^2}{2\sigma_G^2}} d\tau. \quad (6)$$

A recursion relationship for evaluating this function can be found by using integration by parts:

$$\begin{aligned} g_n(x, \sigma_G, t) = & \sigma_G^2 \left[ (n-1)g_{n-2}(x, \sigma_G, t) \right. \\ & \left. - xg_{n-1}(x, \sigma_G, t) + (-t)^{n-1} e^{xt} e^{-\frac{t^2}{2\sigma_G^2}} \right] \quad (7) \end{aligned}$$

for  $n \geq 1$ . The initial function in the series may be evaluated by completing the square in the exponential:

$$g_0(x, \sigma_G, t) = \sqrt{\frac{\pi}{2}} \sigma_G e^{\frac{x^2 \sigma_G^2}{2}} \operatorname{erfc} \left( \frac{x\sigma_G}{\sqrt{2}} - \frac{t}{\sqrt{2}\sigma_G} \right), \quad (8)$$

using the definition of the complementary error function

$$\operatorname{erfc}(y) \equiv \frac{2}{\sqrt{\pi}} \int_y^{\infty} e^{-u^2} du. \quad (9)$$

The terms of the series (Eq. (6)) required to evaluate  $i_G(t)$  may be found using the recursion relationship (Eq. (7)) along with the explicit formula for the first term (Eq. (8)).

### 3. Results from ARCS monitor data

The Gaussian-convolved Ikeda-Carpenter pulse shape derived in Sect. 2 may be used to determine effective source parameters as a function of nominal incident energy by considering the timing diagram Fig. 1. We suppose that the emission time pulse for neutrons near the nominal incident energy may be characterized by the Ikeda-Carpenter function  $i(t_e)$  with source parameters  $\alpha_s$ ,  $\beta_s$  and  $R$ . The neutrons pass through the Fermi chopper and a small fraction are detected by the first beam monitor. If this beam monitor is sufficiently close to the Fermi chopper, this time-of-flight distribution may be parametrized by a Gaussian function (Eq. (3)) located at the center-of-mass flight time  $t_{com}$  to find the effective chopper time width  $\sigma_{m1}$ . At the second beam monitor the source pulse distribution has been reversed in time and the parameters scaled. The intensity as a function of time-of-flight  $t$  may be fit to a Gaussian-broadened Ikeda-Carpenter function  $i_G(t_{com} - t)$  with parameters  $\alpha_{m2}$ ,  $\beta_{m2}$ ,  $R$ , and  $\sigma_{m2}$ . The center-of-mass position takes into account the offset given by Eq. (2) using the as-fit parameters, since this does not change after the convolution.

Based on inspection of Fig. 1, the timing parameters may be scaled by the instrument lengths to provide effective source parameters:

$$\sigma_{m2} = \frac{L_{m2}}{L_{m1}} \sigma_{m1}, \quad (10)$$

$$\alpha_{m2} = \frac{L_{fermi}}{L_{m2} - L_{fermi}} \alpha_s, \quad \text{and} \quad (11)$$

$$\beta_{m2} = \frac{L_{fermi}}{L_{m2} - L_{fermi}} \beta_s. \quad (12)$$

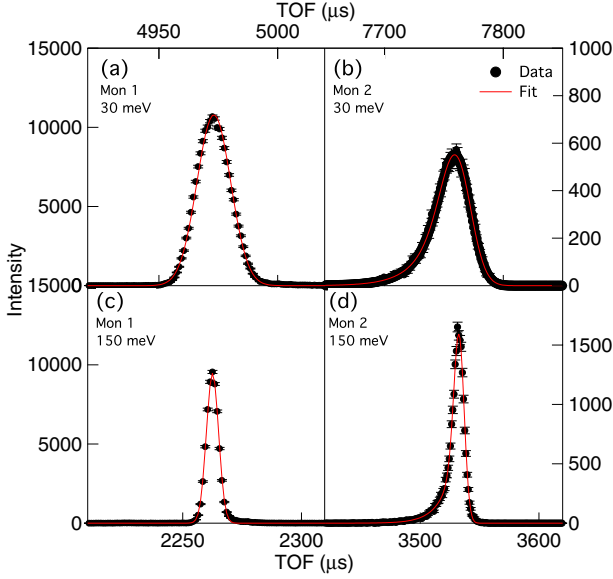


**Figure 2.** ARCS monitor data for 30 meV (a,b) and 150 meV (c,d) nominal incident energy. The first beam monitor is fit to a Gaussian (a,c) and the second to a time-reversed, Gaussian-broadened Ikeda-Carpenter function (b,d).

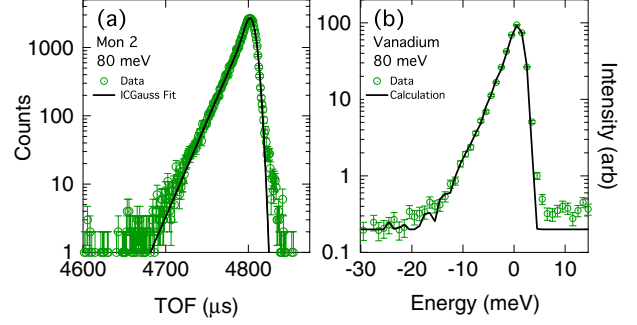
For ARCS the positions of the different components as measured from the source location are  $L_{fermi} = 11.61$  m,  $L_{m1} = 11.835$  m, and  $L_{m2} = 18.50$  m. In addition to these scaling relationships, the results are also corrected for the beam monitor effective thickness along the beam  $l_{mon} = 1$  cm and the histogram bin size  $t_{bin} = 1$   $\mu$ s. The ARCS beam monitor is a low efficiency counter based on  $^3\text{He}$  [2], so it is assumed to provide a flat response over the time it takes the neutrons to pass through it. In the Gaussian approximation, the extra width due to detection uncertainty is taken as

$$\sigma_{det} = \sqrt{\frac{(l_{mon}/v_i)^2 + t_{bin}^2}{12}}, \quad (13)$$

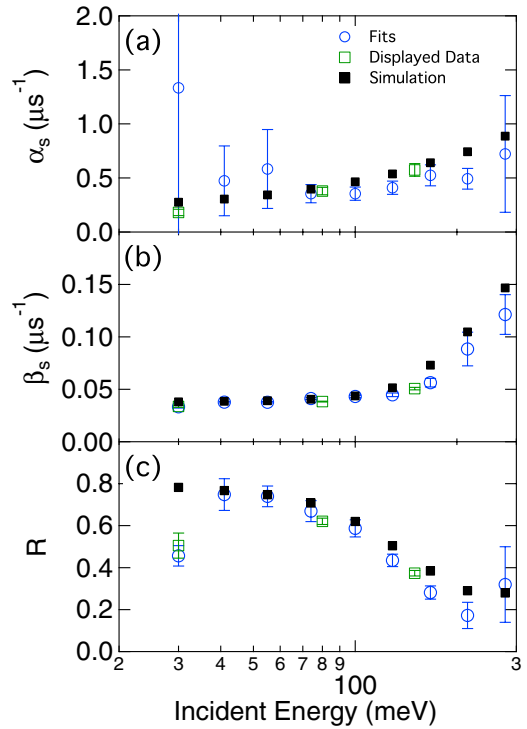
where  $v_i$  is the velocity of the neutrons corresponding to the nominal incident energy. The value of  $\sigma_{det}$  is subtracted in quadrature from  $\sigma_{m1}$  before scaling by Eq. (10). The same value is also added in quadrature to the value of  $\sigma_{m2}$ , since the ARCS monitors have the same thickness and binning in this study.

Figure 2 shows the results of fitting the ARCS monitor data for measurements at 30 meV and 150 meV nominal incident energy. The ARCS 100 meV Fermi chopper was used [4], spinning at 300 Hz and 600 Hz respectively. Data treatment and fitting were performed using Mantid software [5]. Figures 2a and c show Gaussian fits to the first monitor peaks from which  $\sigma_{m1}$  was extracted. The Gaussian approximation provides a reasonable description of the time pulse through the chopper. In Figs. 2b and d the fits to the second beam monitor are displayed. The Gaussian-broadened Ikeda-Carpenter function gives a good parameterization of the asymmetric pulse. The scaled source parameters for these incident energies are plotted in Fig. 4 for comparison to other data.

To check whether the source parameters found from the monitor fitting process corresponded to those needed



**Figure 3.** Comparison of the ARCS second monitor pulse shape (a) and the energy resolution function as measured by vanadium scattering (b) for 80 meV incident energy neutrons. Source parameters were found from the beam monitor data and used to calculate the expected elastic scattering from the ARCS standard vanadium sample.



**Figure 4.** Comparison of the ARCS source parameters as a function of nominal incident energy determined by fits to the beam monitors. Also shown are parameters extracted from Monte Carlo simulations of the SNS target and moderator system.

to explain the overall instrument resolution, a comparison was made to vanadium data. Source parameters for 80 meV incident energy neutrons were taken from the fit to the second beam monitor shown in Fig. 3a, including the chopper pulse time  $\sigma_{m1}$  found from the first monitor data (not shown). The resulting parameters, plotted in Fig. 4, were in turn used to simulate the energy resolution function expected for data taken with the same chopper settings from the ARCS standard vanadium sample (Fig. 3b). The resolution calculation was performed in Tobyfit [6] using the determined source values as well as appropriate information about the Fermi chopper parameters, sample size and instrument geometry. It is clear that the

source parameters provide a good description of the overall width and the asymmetric tail of the resolution function.

The Ikeda-Carpenter source parameters will be energy dependent, with the pulse growing sharper ( $\alpha$ , increasing) and the contribution from the slower term ( $R$ ) decreasing as the incident energy increases [1]. Figure 4 shows the energy dependence of the three extracted source terms from fitting ARCS monitor data for a limited set of runs. Besides the points at 30 meV, 80 meV and 150 meV found from the data plotted in other figures, a separate series of ARCS calibration runs was analyzed in the range from 30 meV to 300 meV. The resulting source parameters are reasonably consistent across this energy range. For higher incident energies, the detection time uncertainty due to the monitor time binning makes using this method less stable. An additional check on the extracted parameters may be made by comparing to the results from Monte Carlo simulations of the SNS target and moderator assembly [7]. The simulation neutrons emerging from the ARCS moderator face were binned by their energy, and the resulting emission time distributions were fit by the Ikeda-Carpenter form (Eq. (1)). In principle there will be a difference between these methods since the beam monitor data sample various neutron energies, as seen by the different slopes of the neutron paths illustrated in the timing diagram Fig. 1, and may be modified by neutron guide effects.

#### 4. Discussion and conclusion

The analysis of the intensity distributions of beam monitors placed in direct-geometry neutron spectrometers provides effective source parameters, which in turn may be compared to source simulations and used as input into calculation of the energy resolution of the instrument as typically measured using incoherent (vanadium) scattering. One advantage of the method is that the beam monitor data are almost always available for measurements of interest since the primary function of the monitors is to check the nominal incident energy by measuring the time-of-flight of the neutron pulses between them. Measurement of the chopper pulse distribution by the first monitor avoids specific assumptions about the chopper transmission function and the effects of neutron guides used in modern chopper spectrometers. It may be expected that this analysis would complement more detailed analytical descriptions of the instrument resolution and full Monte Carlo simulations of scattering experiments.

There are of course limitations to the technique. The thickness of the beam monitors limit their time-of-flight resolution, so for a particular instrument the monitor configuration must be evaluated to see if it is appropriate

for this type of analysis. At higher incident energy, the time binning of the monitors may make extraction of the relevant parameters more difficult. The method ignores correlations beyond the basic ones concerning energy and the time-of-flight. For example, the downstream monitor will typically only intercept the central portion of the beam, so that at lower incident energies for instruments with neutron guides it may miss some of the contribution from higher divergence neutrons. Further work is needed to apply the analysis to other configurations at ARCS as well as extend it to other direct-geometry spectrometers.

For the future, this type of analysis may be extended to a more complete description of the instrument resolution in  $Q$  and  $E$  in a Gaussian approximation while retaining the source asymmetry, an essential feature for many spallation neutron source instruments. An analytic treatment may be quicker for experiment planning or surveying new instrument designs. Having a description of the tail of the resolution could improve the analysis of smaller features near more intense ones. Ultimately the more information that goes into the understanding of the instrument performance, the better one is able to quantify the sample scattering function and discriminate between instrument resolution effects and other sources of background. The goal is a more efficient transformation of neutron scattering data into scientific understanding of the sample under study.

Valuable discussions with Jack Carpenter, Franz Gallmeier and Erik Iverson are gratefully acknowledged. The research at Oak Ridge National Laboratory's Spallation Neutron Source was sponsored by the Scientific User Facilities Division, Office of Basic Energy Sciences, U. S. Department of Energy.

#### References

- [1] S. Ikeda and J. M. Carpenter, Nucl. Instr. and Meth. A **239**, 536 (1985)
- [2] D. L. Abernathy, M. B. Stone, M. J. Loguillo, M. S. Lucas, O. Delaire, X. Tang, J. Y. Y. Lin, and B. Fultz, Rev. Sci. Instrum. **83**, 015114 (2012)
- [3] J. M. Carpenter, *Elements of Slow Neutron Scattering* (unpublished work)
- [4] M. B. Stone, J. L. Niedziela, D. L. Abernathy, L. DeBeer-Schmitt, G. Ehlers, O. Garlea, G. E. Granroth, M. Graves-Brook, A. I. Kolesnikov, A. Podlesnyak, B. Winn, Rev. Sci. Instrum. **85**, 045113 (2014)
- [5] The Mantid Project. <http://dx.doi.org/10.5286/Software/Mantid3.0>
- [6] T. G. Perring, *et al.* See <http://tobyfit.isis.rl.ac.uk>
- [7] F. X. Gallmeier, Spallation Neutron Source report SNS-106100200-TR0195-R00